Hyperspherical close-coupling study of hyperfine transitions in low-energy $p+p\mu$ and $e^{\pm}+$Ps scattering

Akinori Igarashi and Isao Shimamura
The Institute of Physical and Chemical Research (RIKEN), Wako, Saitama 351-0198, Japan

Nobuyuki Toshima
Institute of Applied Physics, University of Tsukuba, Tsukuba 305-8573, Japan

(Received 11 March 1998)

We apply the hyperspherical close-coupling method to the elastic and spin-flip processes in $p+p\mu$ and e^-+Ps (or equivalently, e^++Ps) scattering at low collision energies. The spin-spin interactions V_S are included explicitly in the Hamiltonian, producing the correct hyperfine-splitting energy $\Delta\epsilon$ in the separated-atom limit. A comparison is made with a simpler method in which the effect of V_S is represented only by the symmetry of the wave functions with respect to the interchange of the two identical particles. Explicit inclusion of V_S is found to be of vital importance for the calculation of the spin-flip cross sections for collision energies lower than $\Delta\epsilon$ for both $p+p\mu$ and $e^-(e^+)+$Ps collisions. The elastic cross sections are less sensitive to V_S, but those for $p+p\mu$ are still affected by V_S for collision energies lower than $\Delta\epsilon$. [S1050-2947(98)00908-1]

PACS number(s): 34.80.Bm, 34.80.Nz, 36.10.Dr, 31.15.Ja

I. INTRODUCTION

Knowledge of the spin-flip processes of muonic atoms $p\mu$, $d\mu$, and $t\mu$ in hydrogen-isotope mixtures is important in understanding muon physics such as the physics of muon-catalyzed fusion [1]. Since the mass m_μ of a muon is as large as about 1/9 of the mass m_p of a proton, the picture in which the nuclei are assumed to be almost at rest in comparison with a muon is expected to break down even at low energies. Nevertheless, muonic-atom collisions have been studied mostly by the expansion of the scattering wave function in terms of adiabatic molecular states in a manner similar to the treatment of the ordinary atomic systems [2–4]. Furthermore, corrections that are necessary for the molecular-state representation but negligible in electronic transitions can give rise to a serious effect in the muonic case; the mass used for the molecular states is different from the reduced mass of the muonic atom, and the molecular coordinates fail to tend to the correct Jacobi coordinates in the dissociation limit. These defects cause spurious long-range interactions, which bring about difficulties in solving the scattering equations [5,6]. A large number of adiabatic basis states are required to remedy these difficulties and to achieve convergence in the cross sections [4]. Hu *et al.* [7] solved modified Faddeev equations, instead of using adiabatic molecular basis states, in the calculation of the spin-quenching cross sections for the process $p\mu+p$. They added the atomic hyperfine-splitting energy to the eigenvalue of the upper molecular hyperfine state for approximating the effect of the spin-spin interactions.

The close-coupling method in terms of the hyperspherical coordinates as applied extensively to Coulomb three-body continuum processes has proved to be a very efficient numerical method; see, e.g., Refs. [8–11] and references therein. This hyperspherical close-coupling (HSCC) method has an advantage that the scattering equations contain no nonlocal potentials, which, if present, would complicate the practical calculations significantly. Another advantage is a fast convergence in the scattering parameters as the number of coupled equations is increased. This method has been demonstrated to be very powerful and reliable for the calculations of the cross section for muon transfer between hydrogen isotopes [10]. In the present study, the HSCC method is adopted for the calculations of the elastic and spin-flip cross sections for the $p+p\mu$ collisions for center-of-mass energies of $10^{-3}-10^{2}$ eV. We include the spin-spin interactions explicitly in the Hamiltonian, unlike the work of Ref. [7]. A simplified treatment of the effect of these interactions is also examined. The calculations are extended also for electron scattering by the positronium (Ps) for energies of $10^{-4}-1.0$ eV for further studies of the validity of the adiabatic-basis expansion, which is expected to become more slowly convergent for this equal-mass three-body system. The muon atomic units (m.a.u., in which $\hbar=m_\mu=e=1$) are used for the system $p+p\mu$, and the usual atomic units are used for e^-+Ps.

II. THEORY AND CALCULATION

A. General theory

The present study investigates a three-body system composed of identical particles a_1 and a_2 of a mass M_a and a spin 1/2, and a particle b of a mass M_b and a spin 1/2. The Jacobi coordinates $(\mathbf{R}_i,\mathbf{r}_i)$ $(i=1,2)$ of the system are defined in Fig. 1. After separating out the center-of-mass motion of the total system, one may write the kinetic-energy operator in terms of these Jacobi coordinates as

$$T=-\frac{1}{2M}\nabla_{R_1}^2-\frac{1}{2m}\nabla_{r_1}^2=-\frac{1}{2M}\nabla_{R_2}^2-\frac{1}{2m}\nabla_{r_2}^2 \qquad (1)$$

with $M=M_a(M_a+M_b)/(2M_a+M_b)$ and $m=M_aM_b/(M_a+M_b)$. The total Hamiltonian of the system is given by

$$H=T+V_C+V_S, \qquad (2)$$

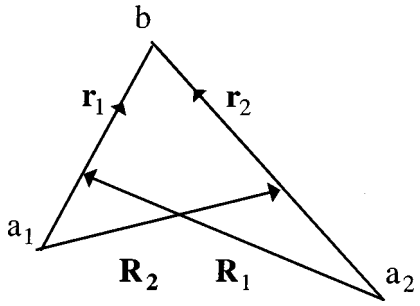

FIG. 1. Jacobi coordinates of the system.

where V_C is the sum of the three two-body Coulomb interactions, and V_S the spin-spin interactions

$$V_S=\lambda\{\delta(\mathbf{r}_1)\mathbf{s}_1\cdot\mathbf{s}_b+\delta(\mathbf{r}_2)\mathbf{s}_2\cdot\mathbf{s}_b\} \tag{3}$$

with the spin operators $\mathbf{s}_1$, $\mathbf{s}_2$, and $\mathbf{s}_b$ of particles a_1, a_2, and b, respectively. The positive-valued constant λ varies depending on the system but is always so small that V_S may be treated as a perturbation.

The $1s$ energy level of a hydrogenlike atom (a_1b) is shifted from the nonrelativistic energy by

$$\frac{1}{2}\lambda|\psi_{1s}(\mathbf{0})|^2\left(F(F+1)-\frac{3}{2}\right) \tag{4}$$

owing to the spin-spin interaction in the first-order approximation. Here, F is the total spin of this atom, i.e., an eigenvalue of the spin operator $\mathbf{s}_1+\mathbf{s}_b$, and ψ_{1s} is the nonrelativistic $1s$ wave function. According to Eq. (4) the spin state $F=0$ has an energy lower than the spin state $F=1$ by

$$\Delta\epsilon=\lambda|\psi_{1s}(\mathbf{0})|^2. \tag{5}$$

Higher-order contributions to the hyperfine splitting have been calculated and compared with precise measurements; see, e.g., Ref. [12]. However, we neglect these higher-order terms for consistency of the whole formulation, since they are negligible, anyway, in the cross-section calculations.

Let

$$\chi^S(a_1,b{:}F,a_2) \tag{6}$$

denote the eigenfunction of the square of the total spin $\mathbf{S}=\mathbf{s}_1+\mathbf{s}_2+\mathbf{s}_b$ with an eigenvalue $S(S+1)$, obtained by coupling the spins $\mathbf{s}_1+\mathbf{s}_b$ and $\mathbf{s}_2$. Since the total Hamiltonian (2) includes no spin-orbit interactions, which are negligibly small for the present collision system because of the dominance of the S-state component, the total spin S is conserved throughout the collision.

For simplicity, here we formulate the theory only for S-wave collisions within a two-state approximation. An extension for multistate expansion and higher partial waves is straightforward. The total wave function of the state $S=1/2$ may be expanded as

$$\begin{aligned}\Psi_{S=1/2}=&\left\{\frac{f_0(R_1)}{R_1}\psi_{1s}(\mathbf{r}_1)\chi^{1/2}(a_1,b{:}0,a_2)\right.\\&\left.-\frac{f_0(R_2)}{R_2}\psi_{1s}(\mathbf{r}_2)\chi^{1/2}(a_2,b{:}0,a_1)\right\}\\&+\left\{\frac{f_1(R_1)}{R_1}\psi_{1s}(\mathbf{r}_1)\chi^{1/2}(a_1,b{:}1,a_2)\right.\\&\left.-\frac{f_1(R_2)}{R_2}\psi_{1s}(\mathbf{r}_2)\chi^{1/2}(a_2,b{:}1,a_1)\right\}.\end{aligned} \tag{7}$$

Note that this wave function is already antisymmetrized for the interchange of the identical particles a_1 and a_2. The radial wave functions f_0 and f_1 are solved under the following two independent asymptotic boundary conditions as $R\to\infty$:

$$\begin{pmatrix}f_0\\f_1\end{pmatrix}\sim\begin{pmatrix}\sin(k_0R)+K_{00}\cos(k_0R)\\(k_0/k_1)^{1/2}K_{10}\cos(k_1R)\end{pmatrix}, \tag{8}$$

and

$$\begin{pmatrix}f_0\\f_1\end{pmatrix}\sim\begin{pmatrix}(k_1/k_0)^{1/2}K_{01}\cos(k_0R)\\\sin(k_1R)+K_{11}\cos(k_1R)\end{pmatrix}, \tag{9}$$

where K_{ij} are elements of the reactance matrix K, and where the momenta k_0 and k_1 satisfy the energy conservation

$$\frac{k_0^2}{2M}=\frac{k_1^2}{2M}+\Delta\epsilon. \tag{10}$$

For collision energies $k_0^2/2M$ lower than $\Delta\epsilon$, the upper channel is closed and the boundary condition reads as

$$\begin{pmatrix}f_0\\f_1\end{pmatrix}\sim\begin{pmatrix}\sin(k_0R)+K_{00}\cos(k_0R)\\0\end{pmatrix}. \tag{11}$$

The K-matrix elements obtained from the above expressions are converted to the cross sections in the standard manner.

For $S=3/2$, the total wave function contains only an $F=1$ component and may be written as

$$\begin{aligned}\Psi_{S=3/2}=&\frac{g(R_1)}{R_1}\psi_{1s}(\mathbf{r}_1)\chi^{3/2}(a_1,b{:}1,a_2)\\&-\frac{g(R_2)}{R_2}\psi_{1s}(\mathbf{r}_2)\chi^{3/2}(a_2,b{:}1,a_1)\\=&\left\{\frac{g(R_1)}{R_1}\psi_{1s}(\mathbf{r}_1)\right.\\&\left.-\frac{g(R_2)}{R_2}\psi_{1s}(\mathbf{r}_2)\right\}\chi^{3/2}(a_1,a_2{:}1,b).\end{aligned} \tag{12}$$

This expression indicates (i) that the spin state $S=3/2$ is spatially antisymmetric with respect to the interchange of the identical particles a_1 and a_2, (ii) that the spin state of these two particles is triplet, and (iii) that no transitions between the hyperfine states can occur for $S=3/2$.

B. Neglect of the spin-spin interactions

The elastic cross sections for $S=3/2$ are expected to be calculated to a good accuracy without the spin-spin interactions, since the spin-flip process is forbidden, and since the energy shift due to the spin-spin interactions is very small. In fact, the spin-spin interactions are negligible even for $S=1/2$ if the collision energy is much higher than the hyperfine splitting, in which case it follows that $k_1 \simeq k_0 (\equiv k)$. Without the spin-spin interactions, the wave function for $S=1/2$ is separable into spatially symmetric and antisymmetric terms with respect to the interchange of a_1 and a_2. The symmetric term corresponds to the singlet state of (a_1, a_2) and the antisymmetric term to the triplet state. This will be understood in the following way.

First, we note the relations

$$\chi^{1/2}(a_1,b:0,a_2)=\frac{1}{2}\chi^{1/2}(a_1,a_2:0,b)-\frac{\sqrt{3}}{2}\chi^{1/2}(a_1,a_2:1,b),$$

$$\chi^{1/2}(a_1,b:1,a_2)=-\frac{\sqrt{3}}{2}\chi^{1/2}(a_1,a_2:0,b)-\frac{1}{2}\chi^{1/2}(a_1,a_2:1,b),$$

$$\chi^{1/2}(a_2,b:0,a_1)=-\frac{1}{2}\chi^{1/2}(a_1,a_2:0,b)-\frac{\sqrt{3}}{2}\chi^{1/2}(a_1,a_2:1,b), \qquad (13)$$

$$\chi^{1/2}(a_2,b:1,a_1)=\frac{\sqrt{3}}{2}\chi^{1/2}(a_1,a_2:0,b)-\frac{1}{2}\chi^{1/2}(a_1,a_2:1,b).$$

We define functions f_+ and f_- by the unitary transformation

$$\begin{pmatrix} f_0 \\ f_1 \end{pmatrix}=\begin{pmatrix} \frac{1}{2} & -\frac{\sqrt{3}}{2} \\ -\frac{\sqrt{3}}{2} & -\frac{1}{2} \end{pmatrix}\begin{pmatrix} f_+ \\ f_- \end{pmatrix}\equiv U\begin{pmatrix} f_+ \\ f_- \end{pmatrix}. \qquad (14)$$

It follows that $U=U^{\dagger}=U^{-1}$ and that

$$\begin{pmatrix} f_+ \\ f_- \end{pmatrix}=U\begin{pmatrix} f_0 \\ f_1 \end{pmatrix}. \qquad (15)$$

Now we may rewrite Eq. (7) in terms of f_+ and f_- as

$$\Psi_{S=1/2}=\left\{\frac{f_+(R_1)}{R_1}\psi_{1s}(\mathbf{r}_1)+\frac{f_+(R_2)}{R_2}\psi_{1s}(\mathbf{r}_2)\right\}\times\chi^{1/2}(a_1,a_2:0,b)+\left\{\frac{f_-(R_1)}{R_1}\psi_{1s}(\mathbf{r}_1)-\frac{f_-(R_2)}{R_2}\psi_{1s}(\mathbf{r}_2)\right\}\chi^{1/2}(a_1,a_2:1,b). \qquad (16)$$

Thus we see that f_+ (f_-) is the radial wave function for the singlet (triplet) channel. The Schrödinger equations for the singlet and triplet channels are uncoupled in the absence of the spin interactions. Therefore, the K matrix in this representation is diagonal and the diagonal elements $K_{\pm}$ are related to the singlet and triplet single-channel phase shifts δ_+ and δ_- by $K_{\pm}=\tan\delta_{\pm}$. The K matrix in the F representation is calculated by the unitary transformation [7]

$$\begin{pmatrix} K_{00} & K_{10} \\ K_{01} & K_{11} \end{pmatrix}=U\begin{pmatrix} K_+ & 0 \\ 0 & K_- \end{pmatrix}U^{\dagger}. \qquad (17)$$

This same unitary transformation of the F channel functions diagonalizes the coupling-potential matrix, as it should [7].

The T-matrix elements for $S=1/2$ are expressible, in the absence of the spin interactions, in terms of the phase shifts δ_+ and δ_- as

$$T_{00}^{S=1/2}=\frac{1}{4}e^{i\delta_+}\sin\delta_+ +\frac{3}{4}e^{i\delta_-}\sin\delta_- ,$$

$$T_{01}^{S=1/2}=T_{10}^{S=1/2}=-\frac{\sqrt{3}}{4}e^{i(\delta_+ +\delta_-)}\sin(\delta_+ -\delta_-), \qquad (18)$$

$$T_{11}^{S=1/2}=\frac{3}{4}e^{i\delta_+}\sin\delta_+ +\frac{1}{4}e^{i\delta_-}\sin\delta_- .$$

The usual spin-averaged elastic cross section σ_e without the spin-spin interactions is obtained as the sum of the absolute-squares of the T matrices for $S=1/2$ and for $S=3/2$ multiplied by each statistical weight:

$$\sigma_e=\frac{4\pi}{k^2}[\tfrac{1}{4}(|T_{00}^{S=1/2}|^2+|T_{10}^{S=1/2}|^2)+\tfrac{1}{4}(|T_{01}^{S=1/2}|^2+|T_{11}^{S=1/2}|^2)+\tfrac{1}{2}\sin^2\delta_-]$$

$$=\frac{4\pi}{k^2}(\tfrac{1}{4}\sin^2\delta_+ +\tfrac{3}{4}\sin^2\delta_-). \qquad (19)$$

In the upper expression of Eq. (19), the four terms containing the T-matrix elements are the contributions from $S=1/2$ and the last term is the contribution from $S=3/2$. The lower expression, which follows from Eq. (18), naturally involves the correct singlet and triplet statistical weights.

C. Hyperspherical close-coupling method

The hyperradius ρ is related to the Jacobi coordinates defined in Fig. 1 as

$$\nu\rho^2=MR_1^2+mr_1^2=MR_2^2+mr_2^2, \qquad (20)$$

with an arbitrary parameter ν having the dimension of mass. The kinetic-energy operator T is expressible as

$$T=-\frac{1}{2\nu}\left(\frac{d^2}{d\rho^2}+\frac{5}{\rho}\frac{d}{d\rho}-\frac{\mathbf{\Lambda}^2}{\rho^2}\right), \qquad (21)$$

where $\mathbf{\Lambda}$ is the five-dimensional grand-angular-momentum operator, whose square may be written as

$$\mathbf{\Lambda}^2 = -\frac{1}{\sin^2\phi_i\cos^2\phi_i}\left(\frac{d}{d\phi_i}\sin^2\phi_i\cos^2\phi_i\frac{d}{d\phi_i}\right) + \frac{\mathbf{L}_{R_i}^2}{\cos^2\phi_i} + \frac{\mathbf{L}_{r_i}^2}{\sin^2\phi_i} \quad (i=1,2), \tag{22}$$

in terms of the hyperangle ϕ_i defined by

$$\tan\phi_i = \frac{\sqrt{m}r_i}{\sqrt{M}R_i} \quad (i=1,2). \tag{23}$$

$\mathbf{L}_{R_i}$ and $\mathbf{L}_{r_i}$ are the angular-momentum operators conjugate to the angles $\hat{\mathbf{R}}_i$ and $\hat{\mathbf{r}}_i$, respectively.

The spin-spin interactions of Eq. (3) may be rewritten in the hyperspherical coordinates as

$$V_S = \frac{\lambda}{4\pi\rho^3}\left(\frac{m}{\nu}\right)^{3/2}\{\delta(\phi_1)\mathbf{s}_1\cdot\mathbf{s}_b + \delta(\phi_2)\mathbf{s}_2\cdot\mathbf{s}_b\}. \tag{24}$$

The ρ^{-3} behavior of the above expression is undesirable at small ρ where the centrifugal potential behaving as ρ^{-2} should be dominant. Because V_S has been introduced to reproduce the small hyperfine splitting in the asymptotic region, the form of V_S at small ρ may be modified to some extent. Thus we introduce a multiplicative cutoff function

$$w(\rho) = 1 - \exp(-d\rho^3) \tag{25}$$

with an arbitrary parameter d to remove the unphysical ρ^{-3} behavior near $\rho=0$. With this modification the Schrödinger equation in the hyperspherical coordinates follows as

$$\left[-\frac{1}{2\nu}\left(\frac{d^2}{d\rho^2}+\frac{5}{\rho}\frac{d}{d\rho}\right) + h_{\rm ad}(\rho,\Omega) - E\right]\Psi(\rho,\Omega) = 0 \tag{26}$$

with

$$h_{\rm ad} = \frac{\mathbf{\Lambda}^2(\Omega)}{2\nu\rho^2} + V_C(\rho,\Omega) + w(\rho)V_S(\rho,\Omega), \tag{27}$$

where Ω represents collectively the five-dimensional angular variable $\omega=(\phi_i,\hat{\mathbf{R}}_i,\hat{\mathbf{r}}_i)$ and the spin coordinates. The adiabatic Hamiltonian $h_{\rm ad}$ contains ρ as a parameter and has eigenfunctions $\{\varphi_j\}$, which also depend on the parameter ρ; the eigenvalue problem reads

$$h_{\rm ad}(\rho,\Omega)\varphi_j(\rho,\Omega) = \left(U_j(\rho) - \frac{15}{8\nu\rho^2}\right)\varphi_j(\rho,\Omega). \tag{28}$$

In the asymptotic limit as $\rho\to\infty$, an adiabatic potential U_j approaches an atomic eigenenergy of either $(a_1 b)$ or $(a_2 b)$, and φ_j describes the corresponding dissociation limit $a_2 + (a_1 b)$ or $a_1 + (a_2 b)$.

The procedure for solving the scattering equation is essentially the same as that used for the muon-transfer problem [10], and will be explained only briefly here. First, the entire region of ρ is divided into a large number of small sectors. Then the total wave function is expanded in the form

$$\Psi(\rho,\Omega) = \sum_j F_j(\rho)\varphi_j(\rho,\Omega) \tag{29}$$

in each sector. If no adiabatic potential has an avoided crossing in a sector, this expansion is used as it is in this sector, similarly to the traditional perturbed-stationary-state expansion. If an adiabatic potential $U_j(\rho)$ has an avoided crossing with another potential $U_k(\rho)$ in a sector, then the corresponding adiabatic functions φ_j and φ_k at a fixed point of ρ, which is chosen to be the midpoint of the sector, are used throughout the sector, similarly to the diabatic-by-sector method. Thus our method is based on a hybrid scheme between the adiabatic and diabatic expansions. By this procedure we can overcome both the difficulties inherent in the adiabatic-basis expansion and the diabatic-by-sector method, namely, the nearly singular character of the nonadiabatic couplings near avoided crossings and the slow convergence of the diabatic-state expansion. The solutions in adjacent sectors are connected smoothly on the boundary between them. The solutions are propagated out in this way to the asymptotic region where all the interactions may be neglected. There the hyperspherical-coordinate representation is transformed into the Jacobi-coordinate representation and the reactance matrix is extracted.

D. Numerical calculations

The adiabatic functions in Eq. (28) are constructed by diagonalizing the adiabatic Hamiltonian $h_{\rm ad}$ at each ρ in terms of Slater-type orbitals. The form of the variational basis functions for total orbital angular momentum L and total spin S is taken as

$$r_1^{\ell_1+n}e^{-\alpha r_1}\cos^{\ell_2}\phi_1\mathcal{Y}^L_{\ell_1\ell_2}(\hat{\mathbf{r}}_1,\hat{\mathbf{R}}_1)\chi^S(a_1,b{:}F,a_2) - r_2^{\ell_1+n}e^{-\alpha r_2}\cos^{\ell_2}\phi_2\mathcal{Y}^L_{\ell_1\ell_2}(\hat{\mathbf{r}}_2,\hat{\mathbf{R}}_2)\chi^S(a_2,b{:}F,a_1), \tag{30}$$

where $\mathcal{Y}^L_{\ell_1\ell_2}(\hat{\mathbf{r}}_i,\hat{\mathbf{R}}_i)$ is a simultaneous eigenfunction of $\mathbf{L}_{r_i}^2$, $\mathbf{L}_{R_i}^2$, and $(\mathbf{L}_{r_i}+\mathbf{L}_{R_i})^2$ with corresponding eigenvalues $\ell_1(\ell_1+1)$, $\ell_2(\ell_2+1)$, and $L(L+1)$. The exponent α in Eq. (30) is carefully chosen to minimize eigenenergies in each sector. 26 s, 21 p, 16 d, and 11 f Slater-type orbitals are used for $pp\mu$, and 18 s, 16 p, 14 d, and 12 f Slater-type orbitals for $e^-e^-e^+$. The corresponding Slater-type orbitals for $p\mu$ and Ps lead to an accuracy of more than ten digits in the energies of all states of these hydrogenlike atoms with a principal quantum number equal to or less than 4. The hyperfine levels are calculated to the leading term by diagonalizing the atomic Hamiltonian with the spin-spin interactions V_S of Eq. (3) included. Analytic expressions for λ in Eq. (3) are found in the literature [13,14]; the $F=1$ state is higher than the $F=0$ state by 0.1823 eV for $p\mu$ and by 8.456×10^{-4} eV for Ps, as compared with values 0.1820 eV [1] and 8.411×10^{-4} eV [12] including higher-order contributions, which are thus found to be negligible for the present purpose.

The coupled radial equations are solved up to $\rho=720$ both for $p+p\mu$ and for e^-+Ps. The entire region [0, 720] is divided into 400 sectors; the sector size is increased gradually, starting from the smallest value 0.1 near the origin out

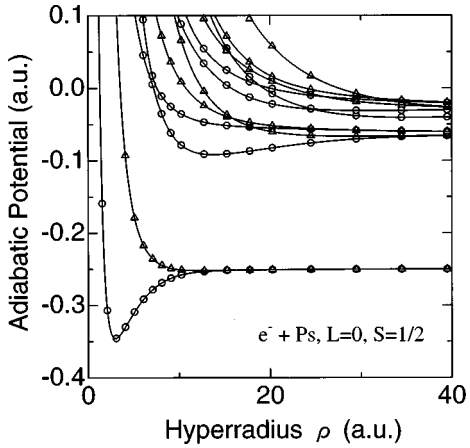

FIG. 2. S-wave adiabatic hyperspherical potentials for the system $e^-e^-e^+$ with the total spin $S=1/2$. Curves represent the results from the calculations including the spin-spin interactions, and the symbols represent those neglecting these interactions. The effect of the spin-spin interactions is too weak to be seen here. ○, singlet electron pair; △, triplet electron pair.

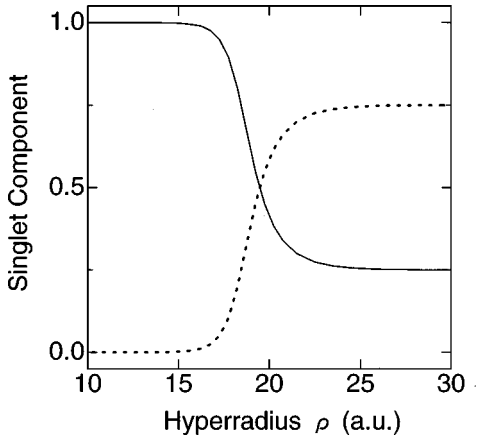

FIG. 3. Singlet components, defined by Eq. (31) in the main text, in the lowest two S-wave channel functions φ_j with $S=1/2$. Solid curve, the lower channel; dotted curve, the upper channel.

to larger-ρ sectors. Two choices, namely, 560 and 720, of the radius for matching between the hyperspherical- and the Jacobi-coordinate representations are tried, and the cross sections are found to differ from each other by less than 1% except near the $F=1$ excitation threshold, where they differ by a few percent. The symmetry of the K matrix is satisfied to better than three digits in the whole energy range studied.

The total wave function is expanded in all the channel functions associated with $p\mu(n=1-3)$ or $\mathrm{Ps}(n=1-3)$ in the dissociation limit. Removal of the channels associated with the states $n=3$ changes the cross sections only by less than 10%, which suggests the convergence much better than 10% since the contributions from even higher states must be smaller.

Two values of 0.5 and 2.0 are chosen for the cutoff parameter d in Eq. (25), and the cross sections are found to be almost independent of the choice of d. This is because the spin-spin interactions are unimportant at small ρ where the dynamics is governed mainly by the three-body Coulomb interactions since the hyperfine splitting is much smaller than the $1s$ orbital energy.

III. RESULTS AND DISCUSSION

A. Adiabatic states

Figure 2 shows some S-wave potential curves of the system $e^-+\mathrm{Ps}$ for $S=1/2$. The potential energies calculated with and without the spin-spin interactions are indistinguishable from each other in the figure. This figure distinguishes between the potential curves of the singlet and triplet electron pairs since they are well defined in the absence of the spin-spin interactions (see Sec. II B). We find pairs of singlet and triplet potential curves, each pair of curves merging together at large ρ. The lowest singlet and triplet curves approach each other around $\rho=20$ and converge asymptotically to the energy of $\mathrm{Ps}(1s)$ at large ρ. Indeed, the hyperfine transition begins to occur around $\rho=20$ as is evident from Fig. 3, which shows the ρ dependence of the singlet components

$$\int d\omega |\langle \chi^{1/2}(a_1,a_2:0,b)|\varphi_j\rangle|^2 \tag{31}$$

in the lowest two adiabatic channel functions φ_j, where the angular brackets indicate the summation over the spin coordinates. The channel function of the lower level is dominated by the singlet component at small ρ, and the singlet component decreases down to the asymptotic value of 1/4 quickly at large ρ. This asymptotic value follows from Eq. (13) and from the fact that the lower channel describes asymptotic fragmentation into $e^-+\mathrm{Ps}(1s,F=0)$. On the contrary, the upper level is dominated by the triplet component at small ρ, and describes asymptotic fragmentation into e^- and $\mathrm{Ps}(1s,F=1)$ with a triplet component of 1/4 at large ρ. The switching between the singlet and triplet states occurs in a region around $\rho=20$. It occurs around $\rho=15$ for the system $p+p\mu$. The spin-spin interactions are negligible at ρ smaller than this transition region.

B. $p+p\mu$ scattering

The energy dependence of the S-wave elastic and spin-conversion cross sections for $S=1/2$ are shown in Figs. 4 and 5 as functions of the center-of-mass collision energy ϵ. The results of the adiabatic-expansion method [4] and the Faddeev-method calculations of Hu *et al.* [7] are also included for comparison. All the three kinds of calculations including the spin-spin interactions are in good agreement.

The elastic cross section $\sigma_{0\leftarrow 0}=(4\pi/k_0^2)|T_{00}^{S=1/2}|^2$ for $F=0$ shows a cusp at the $p\mu(F=1)$ excitation threshold. The cross section σ for one channel close to the threshold ϵ_t of another channel is known to have a cusp if $\sin(2\delta_{\mathrm{th}})>0$, where δ_{th} is the phase shift for the lower channel at ϵ_t, and to decrease rapidly if $\sin(2\delta_{\mathrm{th}})<0$, since

$$\sigma=\begin{cases}\sigma(\epsilon=\epsilon_t)-C|\epsilon-\epsilon_t|^{1/2}2\sin^2\delta_{\mathrm{th}} & \text{for} \quad \epsilon>\epsilon_t \\ \sigma(\epsilon=\epsilon_t)-C|\epsilon-\epsilon_t|^{1/2}\sin(2\delta_{\mathrm{th}}) & \text{for} \quad \epsilon<\epsilon_t\end{cases} \tag{32}$$

with a constant C [15]. Indeed, $\delta_{\mathrm{th}}=0.63$ rad for $p+p\mu(F=0)$ and $\sin(2\delta_{\mathrm{th}})$ is positive, leading to a cusp. The neglect of the spin-spin interactions is a good approximation for the elastic scattering by $p\mu(F=0)$ above the threshold of $p\mu$

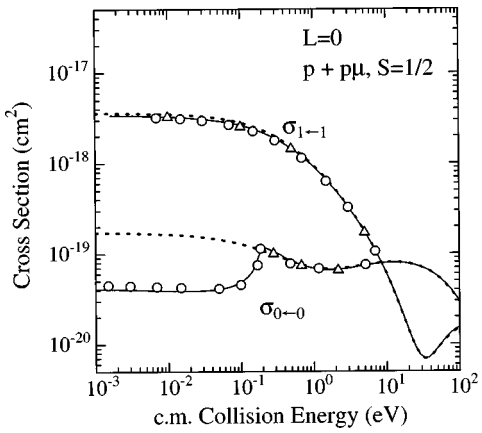

FIG. 4. S-wave elastic cross sections $\sigma_{0\leftarrow 0}$ for $p+p\mu(F=0)$ and $\sigma_{1\leftarrow 1}$ for $p+p\mu(F=1)$ with $S=1/2$. Solid curves, present results including the spin-spin interactions; dotted curves, present results neglecting the spin-spin interactions; ○, the adiabatic-expansion method of Bracci *et al.* (Ref. [4]); △, the Faddeev calculations of Hu *et al.* (Ref. [7]).

$(F=1)$. For elastic scattering $\sigma_{1\leftarrow 1}$ by $p\mu(F=1)$, the neglect of the spin-spin interactions is a good approximation even for lower collision energies.

The cross section $\sigma_{1\leftarrow 0}=(4\pi/k_0^2)(k_1/k_0)|T_{10}^{S=1/2}|^2$ of the spin-flip process, $p+p\mu(F=0)\rightarrow p+p\mu(F=1)$, is found to increase as $\sim\sqrt{\epsilon-\Delta\epsilon}$ from the threshold energy, as is expected [15]. The cross section $\sigma_{0\leftarrow 1}$ of the reverse process decreases as $\sim\epsilon^{-1/2}$ for $\epsilon<$ 0.1 eV, which is also expected from a general theory [16]. The two spin-flip cross sections coincide exactly with each other in the spin-neglecting approximation since there is no energy difference between the $F=1$ and $F=0$ states in this approximation, and hence this approximation is evidently invalid for $\epsilon<\Delta\epsilon$. The effect of the spin-spin interactions diminishes to be negligible above 1 eV, and both $\sigma_{1\leftarrow 0}$ and $\sigma_{0\leftarrow 1}$ converge to the spin-neglected cross section.

No transition between the hyperfine levels is possible for the total spin $S=3/2$; see Sec. II A. The cross section for

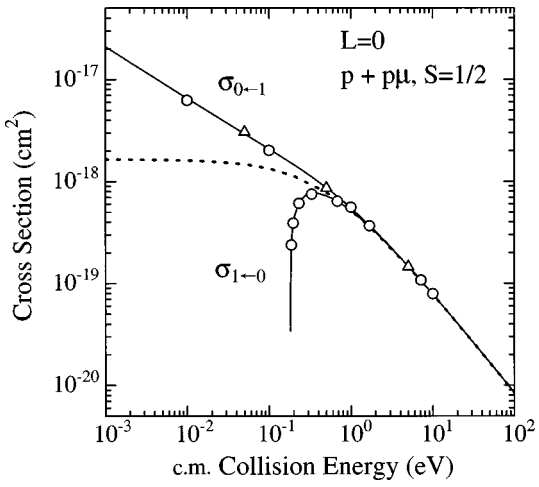

FIG. 5. S-wave spin-flip cross sections $\sigma_{1\leftarrow 0}$ for $p+p\mu(F=0)\rightarrow p+p\mu(F=1)$ and $\sigma_{0\leftarrow 1}$ for $p+p\mu(F=1)\rightarrow p+p\mu(F=0)$ with $S=1/2$. The notations for the curves and the symbols are the same as in Fig. 4.

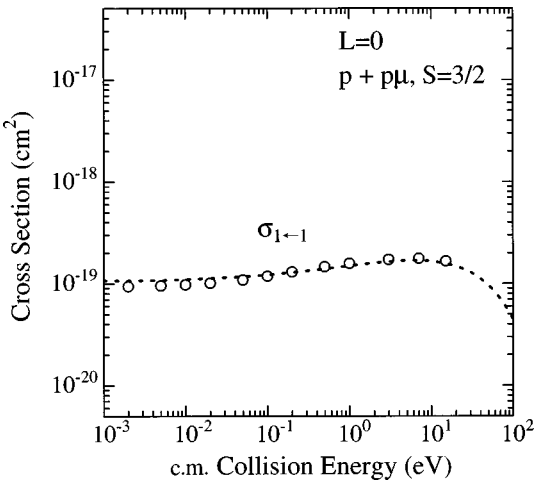

FIG. 6. S-wave elastic cross sections $\sigma_{1\leftarrow 1}$ for $p+p\mu(F=1)$ with $S=3/2$. The notations for the curves and the symbols are the same as in Fig. 4.

elastic scattering $p+p\mu(F=1)$ for $S=3/2$ was obtained from the triplet phase shift calculated without the spin-spin interactions. It is compared in Fig. 6 with the cross section by the adiabatic-expansion method [4], which includes the spin-spin interactions. The two calculations agree well with each other, which corroborates the unimportance of the spin-spin interactions for $S=3/2$ as expected.

C. e^- + Ps scattering

The S-wave elastic cross sections $\sigma_{0\leftarrow 0}(L=0)$ and $\sigma_{1\leftarrow 1}(L=0)$ for e^-+Ps scattering with the total spin $S=1/2$ are compared in Fig. 7 with the S-wave results of the adiabatic-expansion method of Ref. [3]. For scattering from Ps($F=0$), the agreement of the present S-wave calculations with the adiabatic-expansion method is reasonable. However, the Ps($F=1$) elastic cross sections from the adiabatic-expansion

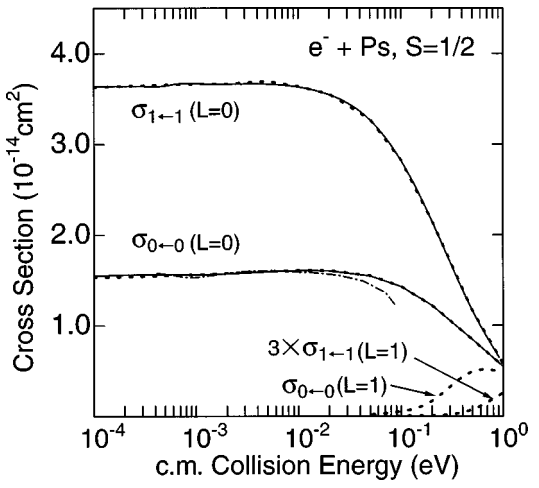

FIG. 7. S- and P-wave contributions to the elastic cross section, $\sigma_{0\leftarrow 0}(L)$ for e^-+Ps($F=0$) and $\sigma_{1\leftarrow 1}(L)$ for e^-+Ps($F=1$), with $S=1/2$. Solid curves, present results including the spin-spin interactions; dotted curves, present results neglecting the spin-spin interactions; dot-dashed curve, the adiabatic-expansion method (Ref. [3]). The cross section $\sigma_{1\leftarrow 1}(L=0)$ by the adiabatic-expansion method is too large to be included in this figure.

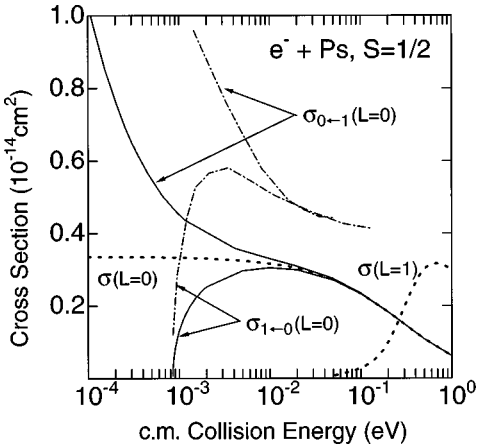

FIG. 8. S-wave spin-flip cross sections $\sigma_{1\leftarrow 0}(L=0)$ for $e^-+\mathrm{Ps}(F=0)\rightarrow e^-+\mathrm{Ps}(F=1)$ and $\sigma_{0\leftarrow 1}(L=0)$ for $e^-+\mathrm{Ps}(F=1)\rightarrow e^-+\mathrm{Ps}(F=0)$ with $S=1/2$, calculated including the spin-spin interactions V_S. The S- and P-wave spin-flip cross sections $\sigma(L)$ calculated neglecting V_S, which are the same for both transitions $F=0\rightarrow 1$ and $F=1\rightarrow 0$, are also shown. The notations for the curves are the same as in Fig. 7.

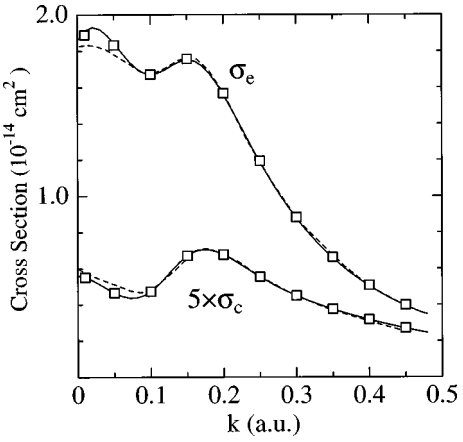

FIG. 9. Spin-weighted total elastic (σ_e) and spin-flip (σ_c) cross sections at wave number k. Solid curves, present results with the basis Ps($n=1-3$); □, present results with the basis Ps($n=1-4$); dashed curves, variational calculation by Ward *et al.* (Ref. [18]).

method (not shown in Fig. 7) are much larger than the present cross sections and show a stronger energy dependence. Since the asymptotic interaction potential decreases as $\sim R^{-4}$ with the distance R between e^- and Ps, the elastic cross sections are expected to be nearly independent of the collision energy at low energies [16], just as for $p+p\mu$ scattering. The unreasonable energy dependence of the elastic $e^-+\mathrm{Ps}(F=1)$ cross sections in Ref. [3] may be attributed to an inadequate description of the wave function for this light-particle system by the adiabatic-expansion method particularly in the asymptotic region; only six adiabatic states are included in the expansion, which may be inadequate for incorporating the nonadiabatic corrections sufficiently or for remedying the drawback that the adiabatic representation fails to satisfy the correct boundary condition in the dissociation limit [5,6,17].

The present $e^-+\mathrm{Ps}(F=0)$ elastic cross section $\sigma_{0\leftarrow 0}(L=0)$ shows a slight decrease at the Ps($F=1$) excitation threshold; the cross section is 1.60×10^{-14} cm^2 at $\epsilon=8.45\times 10^{-4}$ eV and 1.59×10^{-14} cm^2 at $\epsilon=8.46\times 10^{-4}$ eV. The phase shift δ_{th} for the $F=0$ channel at the threshold is -0.0429 rad, which is small and negative. The negative value explains the decrease in the cross section at the threshold, and the small absolute value of $\sin\delta_{\mathrm{th}}$ explains the slightness of the decrease according to Eq. (32). This weak effect of the threshold behavior is the reason for the good performance of the spin-neglecting approximation even for $e^-+\mathrm{Ps}(F=0)$ elastic scattering around the Ps($F=1$) threshold.

The S-wave cross sections $\sigma_{1\leftarrow 0}(L=0)$ and $\sigma_{0\leftarrow 1}(L=0)$ for the spin-flip processes with $S=1/2$ are shown in Fig. 8. The cross sections from the adiabatic-expansion method [3] are about twice as large as the present results. The cross section $\sigma_{0\leftarrow 1}(L=0)$ for the $F=1\rightarrow 0$ transition varies as $\sim\epsilon^{-1/2}$ for $\epsilon<10^{-3}$ eV. The spin-spin interactions are unimportant for $\epsilon>0.05$ eV ($k>0.05$ a.u.), where the two spin-flip cross sections $\sigma_{1\leftarrow 0}(L=0)$ and $\sigma_{0\leftarrow 1}(L=0)$ are nearly equal.

Figures 7 and 8 include the P-wave elastic cross sections $\sigma_{i\leftarrow i}(L=1)$ and spin-flip cross sections $\sigma_{j\leftarrow i}(L=1)$ [denoted by $\sigma(L=1)$ in Fig. 8] calculated without the spin-spin interactions. They become appreciable only above $\epsilon=0.1$ eV, where the neglect of the spin-spin interactions is justified.

The spin-weighted total elastic cross section σ_e is expressible as

$$\sigma_e=\frac{4\pi}{k^2}\sum_{L=0}^{\infty}(2L+1)\left(\frac{1}{4}\sin^2\delta_+^L+\frac{3}{4}\sin^2\delta_-^L\right) \tag{33}$$

in the absence of the spin-spin interactions, as an extension of Eq. (19) for general orbital angular momenta L. Similarly, the spin-averaged spin-flip cross section σ_c takes a form

$$\sigma_c=\frac{\pi}{4k^2}\sum_{L=0}^{\infty}(2L+1)\sin^2(\delta_+^L-\delta_-^L) \tag{34}$$

in the same approximation.

Ward *et al.* [18] calculated the cross sections of $e^-+\mathrm{Ps}$ scattering below the Ps($n=2$) threshold using Eq. (33). They evaluated the S- and P-wave phase shifts by the variational method and estimated the contributions of the higher partial waves by means of a static-exchange model or an adiabatic-exchange model. In the present HSCC calculations, we use two basis sets of different sizes including all the channels dissociating into $e^-+\mathrm{Ps}(n=1-3)$ or $e^-+\mathrm{Ps}(n=1-4)$ and take into account all the partial-wave contributions up to $L=5$, which is high enough to obtain converged cross sections for $k\leqslant 0.5$. The results of Ward *et al.* agree well with the present results for $k>0.1$, as is seen in Fig. 9. The two basis sets in the present calculations lead to cross sections close to each other, which suggests a good convergence.

IV. SUMMARY

We have adopted the hyperspherical close-coupling method to calculate the cross sections for $p+p\mu$ and e^-

+Ps scattering for low energies including and neglecting the spin-spin interactions. The spin-neglected elastic cross sections agree fairly well with the spin-included cross sections for collision energies higher than the hyperfine splitting. For the $e^-e^-e^+$ system, the agreement is good even for energies smaller than the hyperfine splitting.

The neglect of the spin-spin interactions affects the spin-flip cross sections significantly for collision energies at and below the hyperfine-splitting energy. The spin-spin interactions become less and less important as the collision energy increases, and the cross sections for the transitions $F=0 \rightarrow 1$ and $F=1 \rightarrow 0$ merge with each other for collision energies exceeding the splitting energy by an order of magnitude for $p+p\mu$ and by nearly two orders of magnitude for e^- +Ps. The adiabatic-expansion method produces results in good agreement with the present results for the $pp\mu$ system. For the $e^-e^-e^+$ system, however, we find serious disagreement between the adiabatic-expansion cross sections of Ref. [3] and the present results.

[1] J. S. Cohen, in *Review of Fundamental Processes and Applications of Atoms and Ions*, edited by C. D. Lin (World Scientific, Singapore, 1993), p. 61.

[2] S. S. Gershtein, Zh. Éksp. Teor. Fiz. **34**, 463 (1958) [Sov. Phys. JETP **34**, 318 (1958)].

[3] V. S. Melezhik and F. R. Vukajlović, Phys. Rev. Lett. **59**, 641 (1987).

[4] L. Bracci, C. Chiccoli, G. Fiorentini, V. S. Melezhik, P. Pasini, L. I. Ponomarev, and J. Wozniak, Muon Catal. Fusion **4**, 247 (1989).

[5] J. B. Delos, Rev. Mod. Phys. **53**, 287 (1981).

[6] A. Macías and A. Riera, Phys. Rep. **90**, 299 (1982).

[7] C. Y. Hu, A. A. Kvitsinsky, and J. S. Cohen, J. Phys. B **28**, 3629 (1995).

[8] J.-Z. Tang, S. Watanabe, and M. Matsuzawa, Phys. Rev. A **46**, 2437 (1992); J.-Z. Tang and I. Shimamura, *ibid*. **50**, 1321 (1994); **51**, R1738 (1995); **52**, R3413 (1995); A. Igarashi and I. Shimamura, *ibid.* **56**, 4733 (1997).

[9] A. Igarashi and N. Toshima, Phys. Rev. A **50**, 232 (1994).

[10] A. Igarashi, N. Toshima, and T. Shirai, Phys. Rev. A **50**, 4951 (1994).

[11] Y. Zhou and C. D. Lin, J. Phys. B **27**, 5065 (1994); Phys. Rev. Lett. **75**, 2296 (1995).

[12] G. S. Adkins, R. N. Fell, and P. M. Mitrikov, Phys. Rev. Lett. **79**, 3383 (1997); A. H. Hoang, P. Labelle, and S. M. Zebarjad, *ibid*. **79**, 3387 (1997).

[13] B. H. Bransden and C. J. Joachain, *Physics of Atoms and Molecules* (Longmans, London, 1983), p. 235.

[14] V. B. Berestetskii, E. M. Lifshitz, and L. P. Pitaevskii, *Quantum Electrodynamics*, 2nd ed. (Pergamon, Oxford, 1982), Sec. 84.

[15] L. D. Landau and E. M. Lifshitz, *Quantum Mechanics*, 3rd ed. (Pergamon, Oxford, 1977), Sec. 147.

[16] *Quantum Mechanics* (Ref. [15]), Sec. 143.

[17] V. S. Melezhik, L. I. Ponomarev, and M. P. Faifman, Zh. Éksp. Teor. Fiz. **85**, 434 (1983) [Sov. Phys. JETP **58**, 254 (1983)].

[18] S. J. Ward, J. W. Humbertson, and M. R. C. McDowell, J. Phys. B **20**, 127 (1987).